

133

LONG TERM HIGH TEMPERATURE CORROSION STUDIES OF  
HIGH TEMPERATURE ALLOYS IN CHLORINE CONTAMINATED ENVIRONMENTS

by

M. H. RHEE, M. J. McNALLAN, and M. F. ROTHMAN

Reprinted from:

# High Temperature Corrosion in Energy Systems

Proceedings of the symposium co-sponsored by the Joint Corrosion and Environmental Effects Committee of The Metallurgical Society of AIME and the Materials Science Division of the American Society for Metals; the High Temperature Alloys Committee of The Metallurgical Society of AIME; The Energy and Resources Committee of the Material Science Division; and the American Society for Metals Energy Division.

Edited by  
**Michael F. Rothman**  
*Cabot Corporation*  
Kokomo, Indiana

CONFERENCE  PROCEEDINGS

*The Metallurgical Society of AIME*

LONG TERM HIGH TEMPERATURE CORROSION STUDIES OF HIGH TEMPERATURE ALLOYS

IN CHLORINE CONTAMINATED ENVIRONMENTS

M. H. Rhee, M. J. McNallan, M. F. Rothman\*  
Department of Civil Engineering, Mechanics, and Metallurgy  
University of Illinois at Chicago  
P.O. Box 4348  
Chicago, IL 60680

\*Technology Department  
Cabot Corporation  
Kokomo, IN 46901

High temperature chlorine contaminated environments may be encountered in a number of modern industrial and energy conversion systems. Such environments have been shown to be extremely severe from a corrosion control standpoint. Rather little information is available on the corrosion properties of alloys in these environments, and the bulk of this information has been obtained in short term tests (24 hours or less). This paper will report the results of a series of high temperature corrosion tests performed on superalloys for periods up to 400 hours in an oxidizing environment consisting of argon containing 20% oxygen and 0.25% chlorine at 900°C.

## Introduction

High temperature chlorine containing environments are among the most severely corrosive environments which can be encountered in industrial processes. The behavior of metals and alloys in chlorinating environments is not well known in spite of the increasing number of processes which produce such environments, including the incineration of municipal wastes<sup>1,2</sup>, the combustion of chlorine contaminated coal<sup>3</sup>, and waste heat recuperation from chemical and metallurgical processes which utilize chlorine as a reactant.<sup>4</sup>

The majority of the information which is readily available for high temperature chlorine accelerated corrosion is based upon the results of field tests in which the thermodynamic conditions producing the corrosion are not well controlled, or short term (50 hours or less) laboratory tests<sup>5-9</sup>. Laboratory tests performed in pure  $\text{Cl}_2$  or  $\text{HCl}$  are not likely to adequately predict materials performance in mixed industrial environments where additional oxidizing species such as oxygen and sulfur are also present. Furthermore, recent experiments have shown that the kinetics of chlorine accelerated corrosion reactions often do not follow regular linear or parabolic rate laws, so that the extrapolation of the results of short term experiments may lead to the overestimation or underestimation of the extent of corrosion which is encountered in practice.<sup>10</sup>

In this study, the performance of a number of commercial high temperature alloys has been studied for periods up to 400 hours in an environment consisting of argon containing 20% oxygen and 0.25% chlorine by volume. These conditions were selected after earlier experiments demonstrated that test coupons of several of the alloys could not survive 400 hours of exposure to a more corrosive environment.<sup>11</sup>

## Apparatus and Procedures

The apparatus used in these tests has been described elsewhere, and is shown schematically in Figure 1<sup>11</sup>. It consists of a fused quartz reaction tube, and a fused quartz rack from which the specimens are suspended. Reactive gases were purified by passage through dessicant columns before being mixed and supplied to the furnace through the center of the sample rack. The gases are heated to the furnace temperature and distributed over the cross section of the reaction tube by passing them through a bed of packed, crumbled firebrick (Babcock and Wilcox K-30) at the bottom of the reaction tube.

The sample rack was designed with a knowledge of the importance of volatile corrosion product species in high temperature halogen corrosion. The corrosive gas mixture travelled upwards through the furnace with a superficial velocity of 1.5cm/sec. The samples were mounted at least 1 cm apart on a plane orthogonal to the direction of flow of the gases to prevent the inadvertant cross contamination of the specimens by gaseous or liquid corrosion products. Volatile corrosion products condensed on the water cooled cap at the top of the furnace, while condensed corrosion products either remained on the specimens or collected at the bottom of the reaction tube.

Metal specimens were in the form of one to two mm thick sheet cut into square coupons approximately one cm on a side. The compositions of the alloys included in this study are shown in Table I. The metals were supplied in the solution heat treated state with the exceptions of alloy R-41 and alloy 263 which were in the fully heat treated condition. The

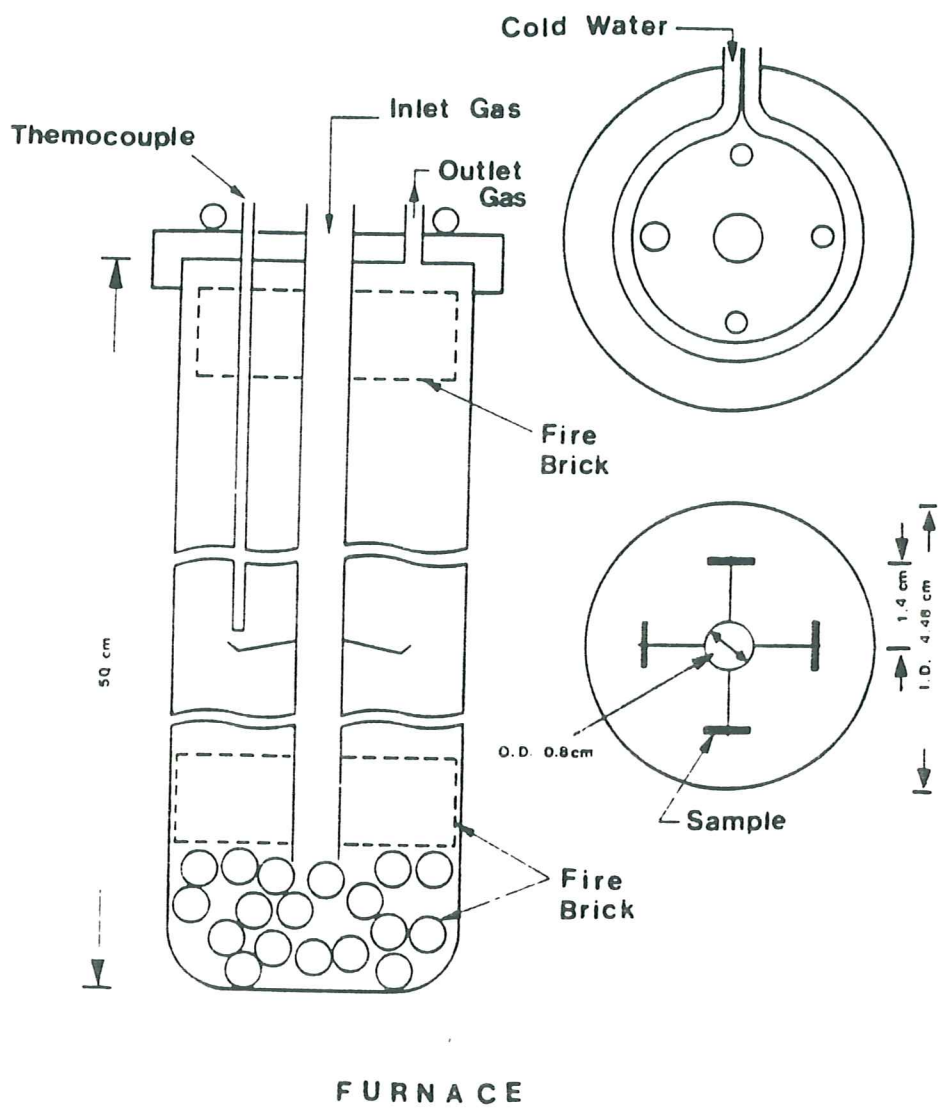


Figure 1. Schematic diagram of apparatus used for long term tests of high temperature alloys in chlorine containing environments.

TABLE I

## NOMINAL COMPOSITIONS OF ALLOYS (Wt.%)

<u>Alloy</u>	<u>Ni</u>	<u>Fe</u>	<u>Co</u>	<u>Cr</u>	<u>Mo</u>	<u>W</u>	<u>Si</u>	<u>Mn</u>	<u>Al</u>	<u>Ti</u>	<u>C</u>	<u>others</u>
HASTELLOY alloy X	Bal.	19	1.5	22	9	0.6	1*	1*	-	-	0.1	
HASTELLOY alloy S	Bal.	3*	-	16	15	-	0.5	0.5	-	-	.02*	.009B, .02La
HASTELLOY alloy C-276	Bal.	5	-	16	16	4	.08*	1*	-	-	.01*	
CABOT alloy No. 214	Bal.	4	-	16	-	-	-	-	4.2	-	.05	.01Y
CABOT alloy No. 600	Bal.	8	-	16	-	-	0.5*	1*	-	-	.04	
CABOT alloy No. 625	Bal.	5*	-	21	9	-	0.5*	0.5*	0.4*	0.4*	.04	3.5Cb
CABOT alloy No. 800H	33	Bal.	-	21	-	-	1	1.5*	0.4	0.4	.08	
CABOT alloy No. R-41	Bal.	5*	11	19	10	-	0.5*	1*	1.5	3	.10	.006B
CABOT alloy No. 263	Bal.	0.7*	20	20	6	-	0.4*	0.6*	0.4	2.2	.06	
HAYNES alloy No. 188	22	3*	Bal.	22	-	14	0.4	1.5*	-	-	.10	.04La
HAYNES alloy No. 556	20	Bal.	18	22	3	2.5	0.4	1*	0.2	-	.10	.8Ta, .2N, .02La, .02Zr
Type 310 Stainless Steel	19	Bal.	-	25	-	-	.5	.8	-	-	.10	
INCONEL alloy No. 601	Bal.	14	-	23	-	-	0.5*	1*	1.4	.3	.10*	

HASTELLOY, CABOT, AND HAYNES are registered trademarks of Cabot Corporation. INCONEL is a registered trademark of the Inco family of companies.

\* Maximum

thirteen alloys were tested in groups of four with alloy R-41 included in each group as a control to demonstrate the reproducibility of the environments.

In each test, the alloys were suspended in the furnace and the furnace was purged with argon before being heated to the test temperature. When the desired temperature was reached, the corrosive gas mixture was allowed to replace the argon and the environment was maintained for 50 hours. At the end of 50 hours, the furnace was purged with argon again, and the samples were cooled, removed from the furnace, and weighed and photographed. This procedure was repeated until the total time of exposure was 400 hours. This test procedure therefore, produces long term exposure with infrequent thermal cycling in which the temperature changes always occur in an inert environment.

#### Weight Change Results and External Corrosion Products

The weight change behavior exhibited by the alloys exposed in each of the four runs is illustrated in Figures 2 through 5 respectively. The results show approximately linear decreases in mass for all of the alloys with the exception of alloy 214 which shows a slight increase in mass during the first 100 hours of exposure. This indicates that the principal corrosion products in this environment are volatile chloride species. After each 50 hour period of exposure, deposits of chlorides were removed from the water cooled cap at the top of the furnace. Especially large amounts of deposits were found during test number 4 where several of the alloys showed large decreases in mass. Only very small amounts of material were found at the bottom of the furnace at the conclusions of the experiments, indicating that the condensed corrosion products remained on the specimens during cooling. The scale of corrosion products on the specimens was very porous and friable, and some material was lost when the specimens were handled during the weighing process. Figure 6 shows the variation in the mass of the alloy R-41 specimens during each of the four tests. The reproducibility of the change in mass with time for these specimens is within 10%, and no significant effects of cross contamination could be detected.

The linear decrease in the mass of the specimens with time observed in these tests is consistent with the parabolic kinetics of corrosion observed for high temperature alloys in a more corrosive environment<sup>11</sup> and for pure nickel and cobalt<sup>12,13</sup> in the same environment in shorter term tests. In this form of corrosion, a scale of oxide corrosion products forms on the metal specimens and is subsequently attacked by chlorine leaving a porous, non-protective scale. The period during which the mass of the specimens increases with time is only a few hours long, and cannot be distinguished in long term tests such as this one.

The alloy which shows the least attack in this environment is alloy 214. This alloy contains the highest concentration of aluminum of any of the alloys in this study, and forms an oxide scale which consists primarily of aluminum oxide. INCONEL alloy No. 601, which contains a lower, but still significant concentration of aluminum, showed substantially less weight loss than alloy 600 which otherwise has a similar composition, despite the fact that it does not form a continuous alumina film. The vapor pressure of  $AlCl_3$  in equilibrium with  $Al_2O_3$  and the test environment is very low, and the  $Al_2O_3$  rich scale which forms on alloy 214 appears to protect the underlying nickel and chromium rich metal from attack. The relatively poor performance of the titanium oxide and chromium oxide forming alloys in these tests indicates that these oxides are less effective in

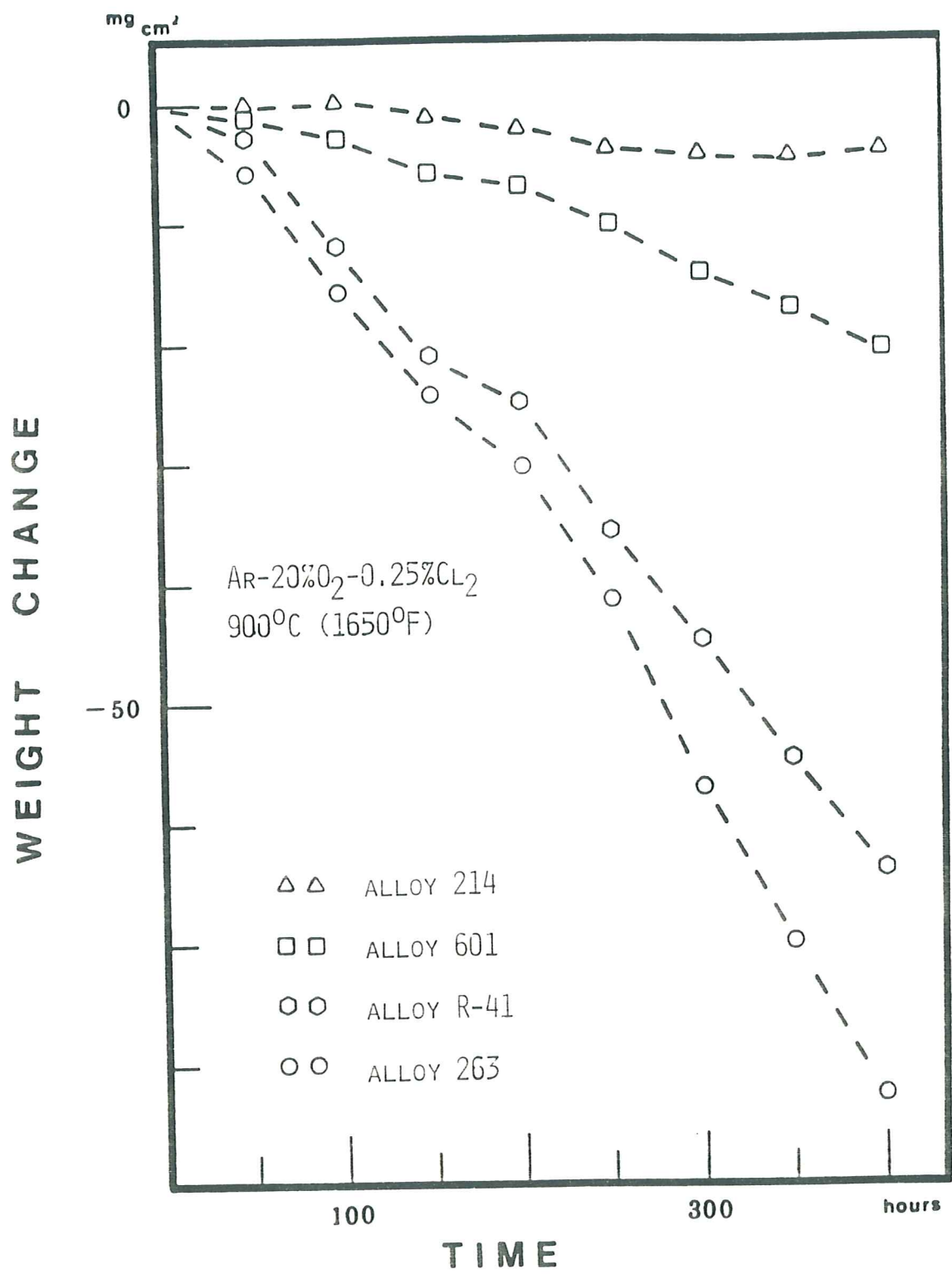


Figure 2. Weight change data from Run #1. Alloy 214, alloy 601, alloy 263, and alloy R-41.

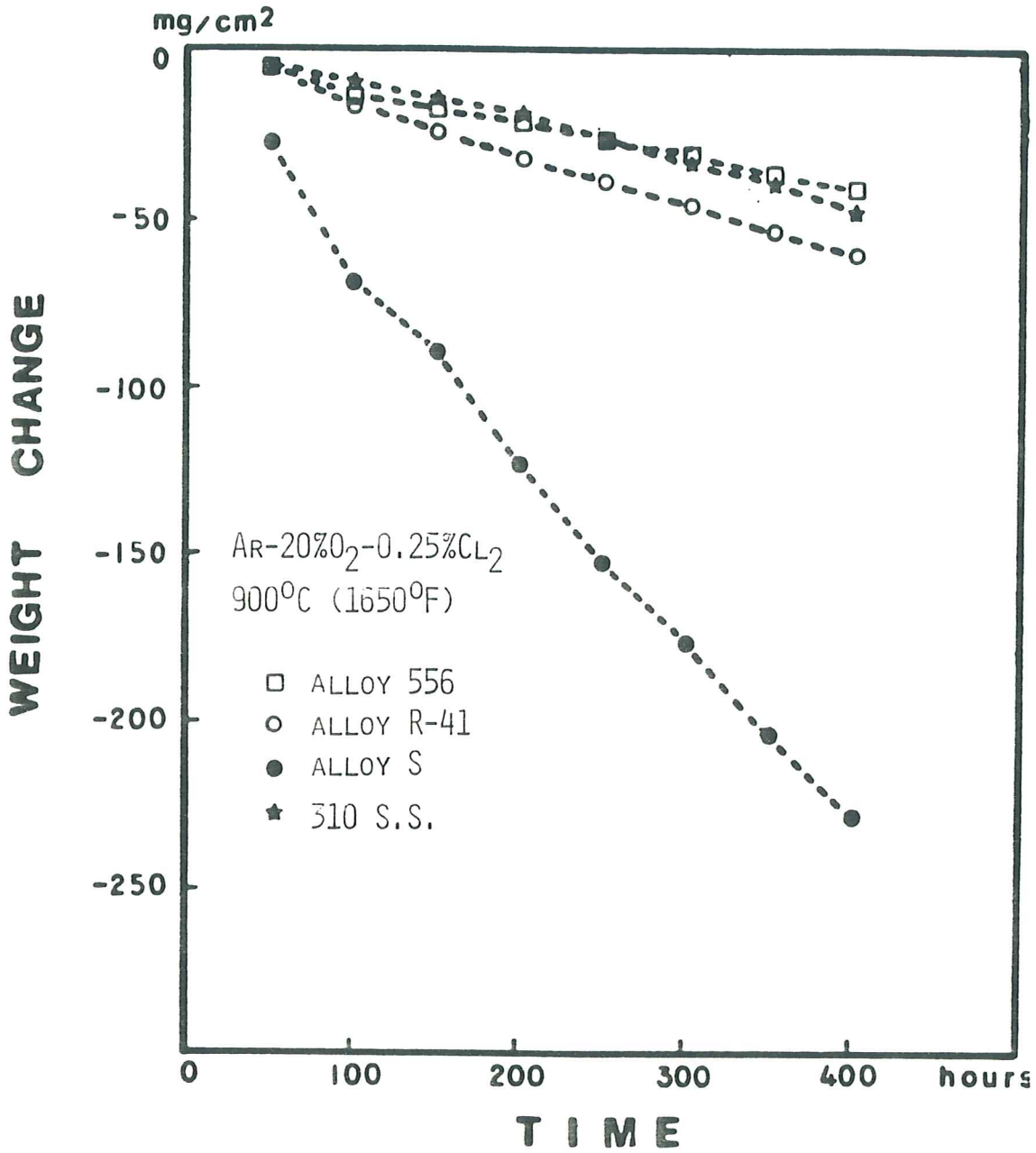


Figure 3. Weight change data for Run #2. Alloy 556, alloy S, 310 stainless steel, and alloy R-41.



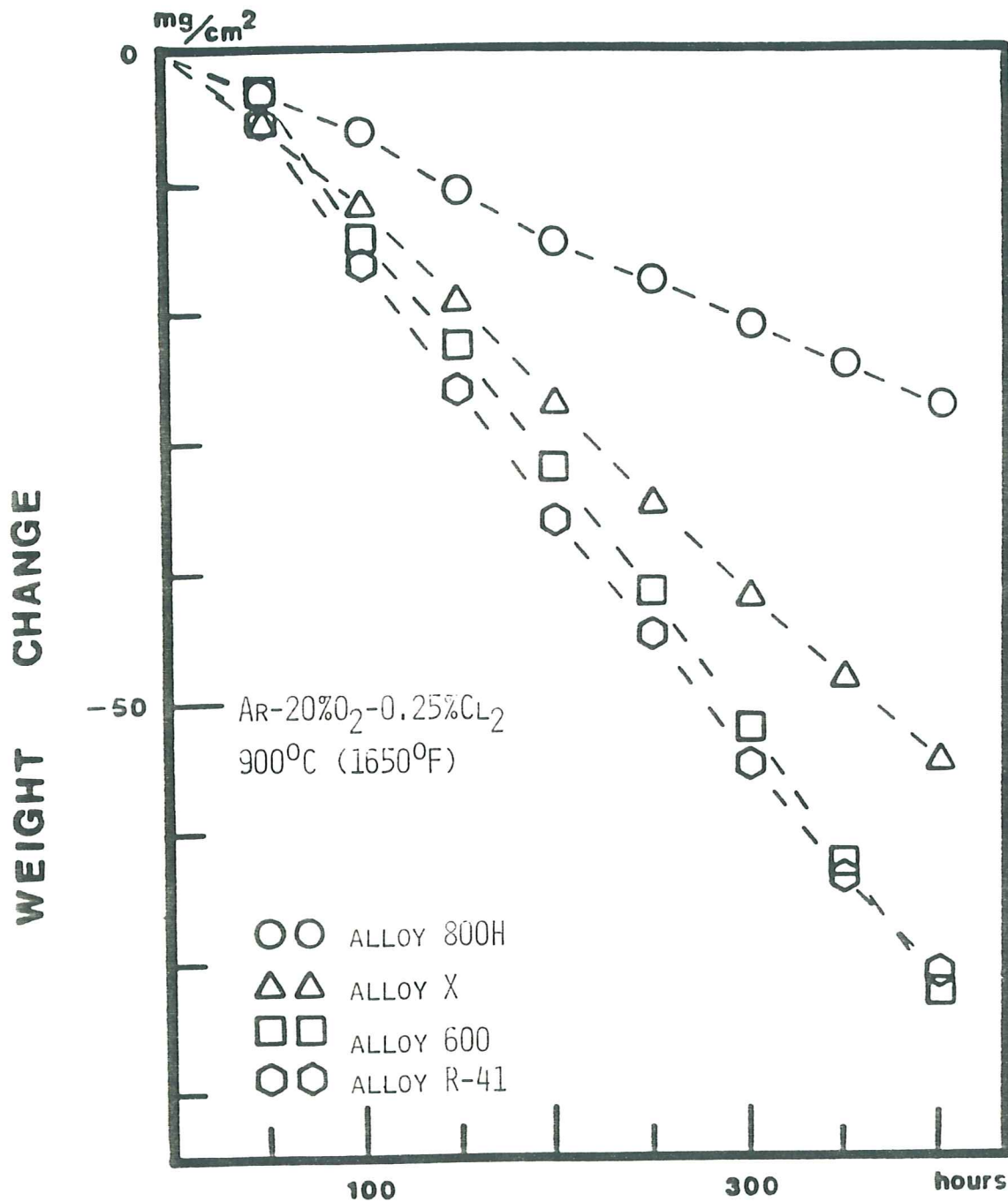


Figure 4. Weight change data for Run #3. Alloy 800H, alloy X, alloy 600, alloy R-41.

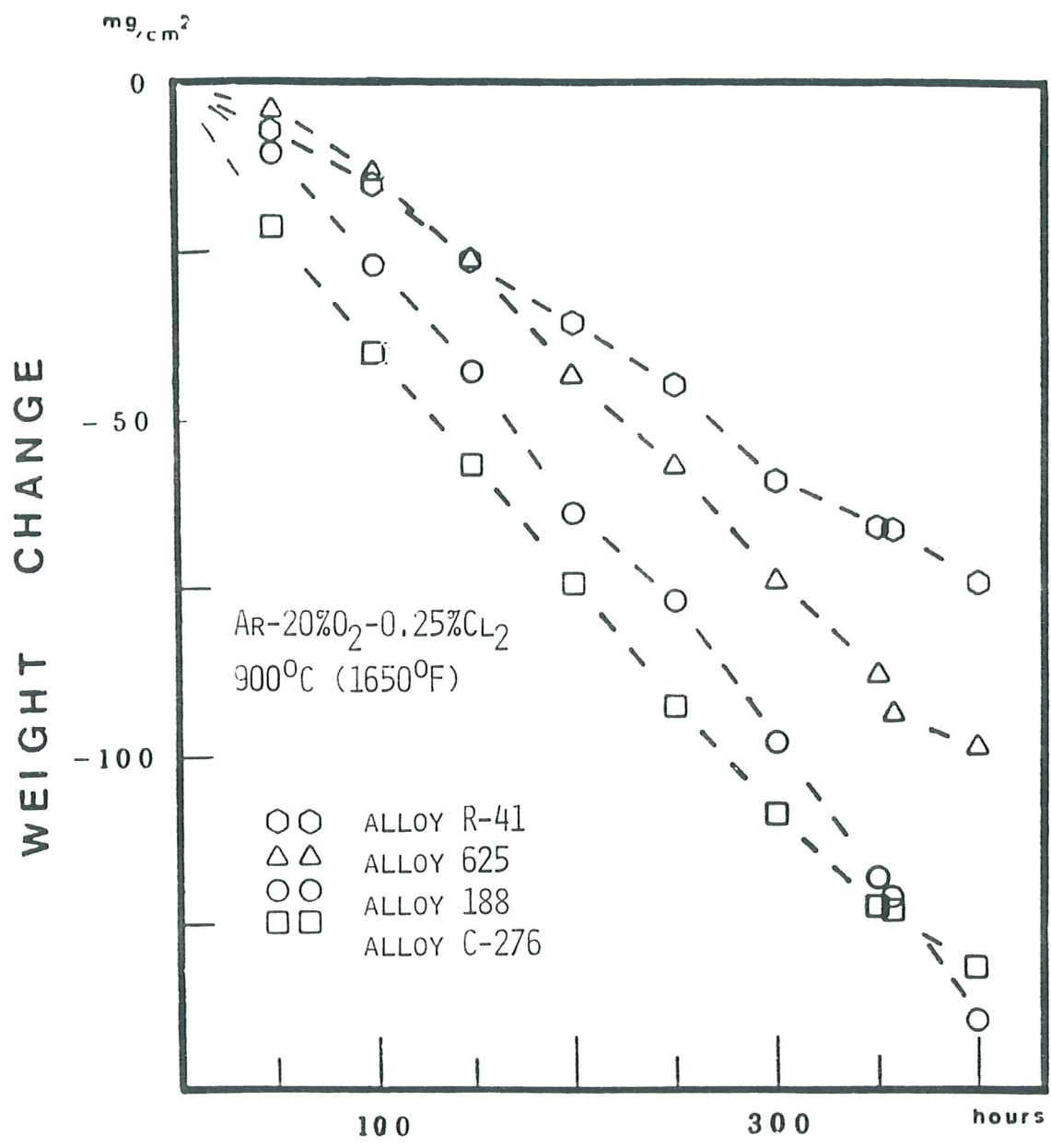


Figure 5. Weight change data from Run #4. Alloy 625, alloy 188, alloy C-276, alloy R-41.

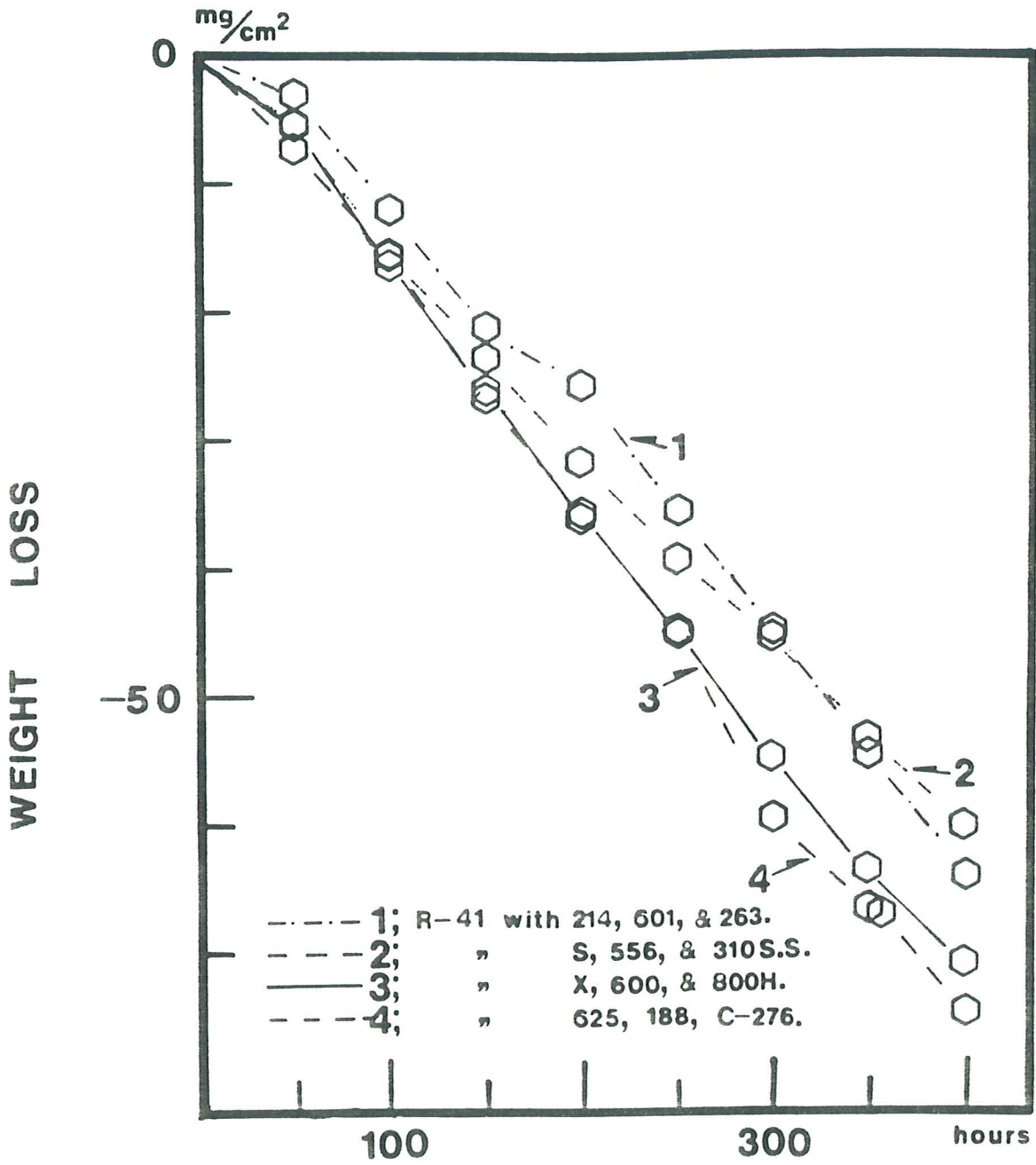


Figure 6. Weight change data for alloy R-41 specimens in all four runs.

protecting the metals from chlorine.

The second ranking materials in terms of weight loss were the iron base alloys: HAYNES alloy No. 556, alloy 800H, and 310 stainless steel. Iron forms a more stable oxide than does either nickel or cobalt, and therefore the vapor pressure of iron chloride is lower than that of nickel or cobalt chloride in environments where the oxides are thermodynamically stable. Figure 7 shows a scanning electron micrograph of the scale which formed on HAYNES alloy No. 556 along with some representative semi-quantitative analyses obtained by energy dispersive X-ray analysis. No chlorine is detected in the corrosion product scale on the specimen which consists largely of chromium oxide and contains outcroppings which are enriched in tantalum and iron. The concentrations of both nickel and cobalt in the scale are much lower than the corresponding concentrations of these elements in the base metal.

The alloys which are attacked most severely in this environment are the cobalt and nickel based alloys which contain high concentrations of tungsten or molybdenum: notably HAYNES alloy No. 188, HASTELLOY alloy S, HASTELLOY alloy C-276, and alloy No. 625. Both tungsten and molybdenum form stable oxychlorides which will have very high vapor pressures in this environment. Figure 8 shows a scanning electron micrograph of the surface of the HASTELLOY alloy S specimen at a position where a portion of the oxide scale has spalled after removal from the furnace. Again, no chlorine is detected in the corrosion product scale. The composition in region 1, where the scale had spalled to reveal the underlying metal, is very close to the nominal composition of the alloy. The oxide scale in regions 2 and 3 is enriched in chromium and iron, depleted in nickel, and contains virtually no molybdenum.

#### Internal Penetration and Total Corrosive Attack

At the conclusion of the 400 hours of exposure, all of the specimens were sectioned and mounted for metallographic examination. Figure 9 shows cross sectional views of several of the alloys. Each photograph has been cropped to the original thickness of the metal specimen, so that the distance between the exterior surface of the specimen in the figure and the outside of the photograph corresponds to the metal loss by oxidation and volatilization. The attack occurs by uniform metal wastage, by pitting attack, and by internal attack. The specimen of alloy 625 shows a clear example of metal wastage, with only minimal internal attack very near the corroding interfaces. The specimen of INCONEL alloy 601 shows primarily pitting type attack along with somewhat more severe internal attack concentrated along the grain boundaries. The specimen of HAYNES alloy No. 188 shows very severe uniform attack as well as internal attack which penetrates through to the center of the specimen. The specimen of alloy 214 shows virtually no uniform metal wastage with all of the attack occurring along the grain boundaries.

The metallographic examinations revealed substantial internal attack in nearly all of the specimens. The degree of internal penetration varied from one alloy to another, and was often least severe in the alloys which showed the most severe metal loss attack. Figure 10 shows the total depth of metal affected by corrosion after 400 hours of exposure to the environment for all of the alloys included in the study. The metal wastage for each specimen is indicated by the dotted line on the bar graph, while the end of the bar indicates the average depth of penetration of the internal attack. No depth of internal attack could be determined for alloy 188 because the internal attack penetrated through the center of the

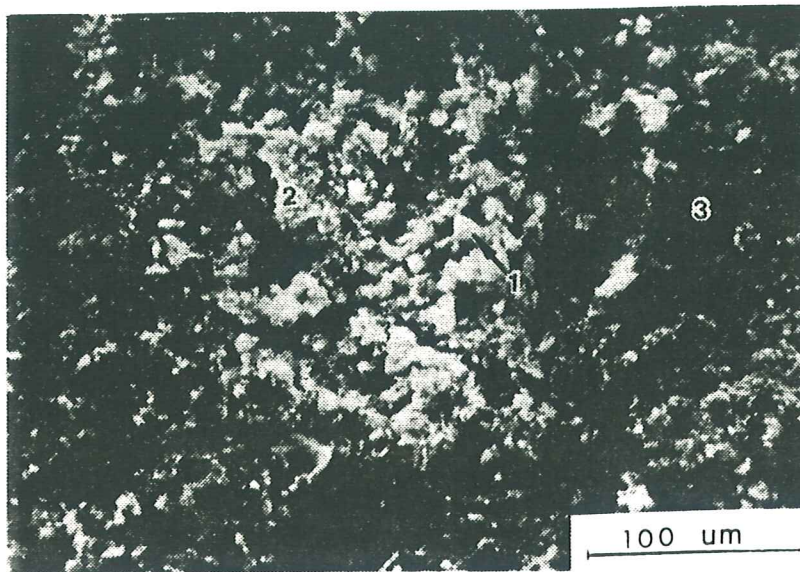


Figure 7. Corrosion product scale formed on alloy 556 after 400 hours of exposure. Semi-quantitative energy dispersive X-ray analyses.

Position	%Al	%Co	%Cr	%Fe	%Nb	%Ni	%Ta	%W
1	0.23	0.03	43.25	13.95	1.58	3.49	36.38	0.98
2	0.09	0.04	80.89	5.95	0.42	1.56	1.11	9.89
3	0.07	0.04	94.93	2.06	0.17	0.35	2.09	-

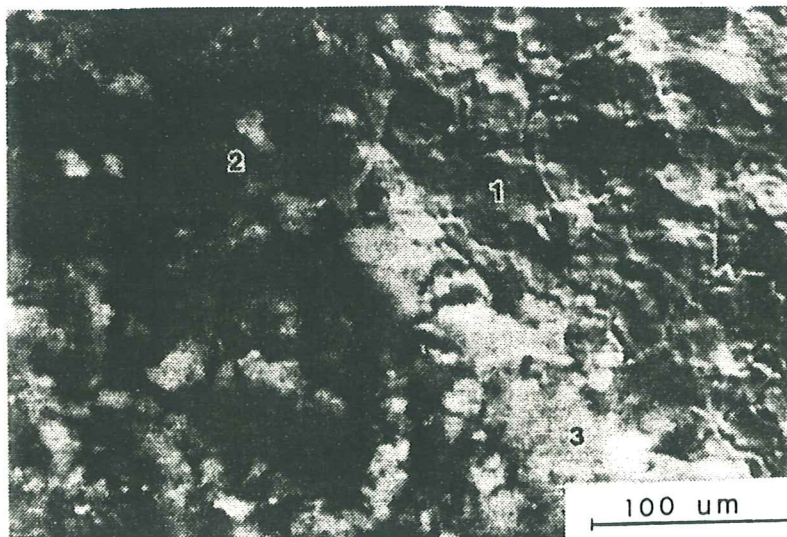
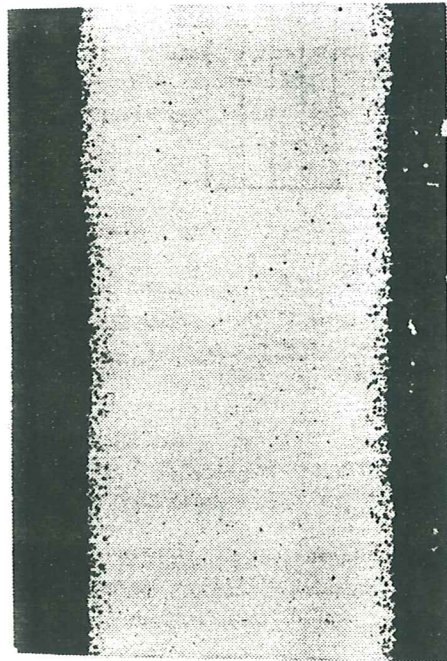
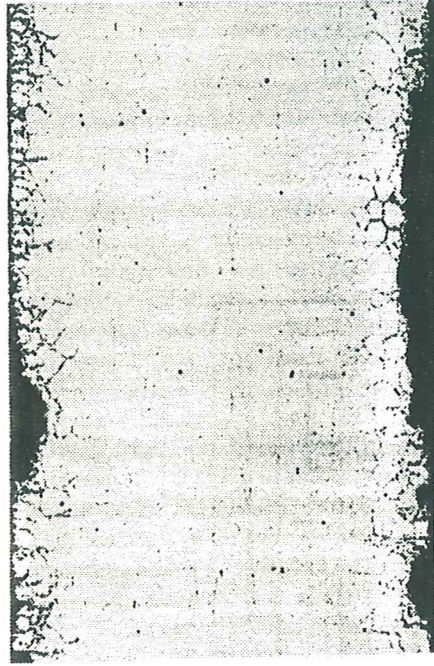


Figure 8. External surface of alloy S specimen after 400 hours of exposure showing region of spalled oxide. Semi-quantitative X-ray analyses.

Position	%Al	%Cr	%Fe	%Mo	%Ni	%Si
1	0.18	17.02	1.04	10.66	70.68	0.39
2	0.32	59.24	17.92	0.44	19.48	2.54
3	0.89	53.20	16.35	0.84	24.63	0.39

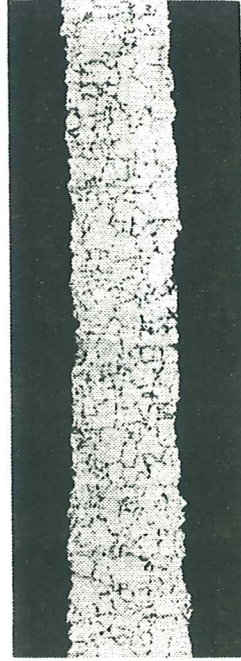


alloy 625

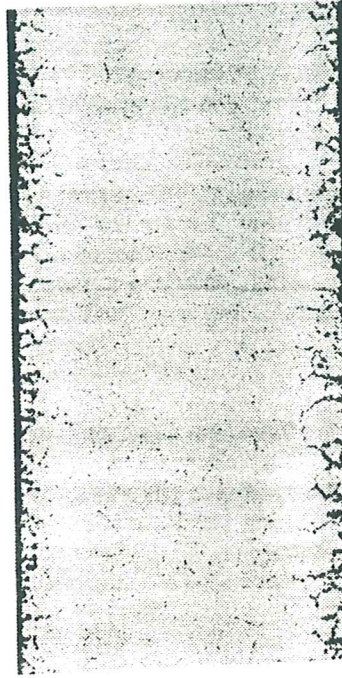


alloy 601

200  $\mu$



alloy 188



alloy 214

Figure 9. Optical micrographs of cross sections of alloys after 400 hours of exposure. Width of photograph corresponds to original thickness of specimen in each case.

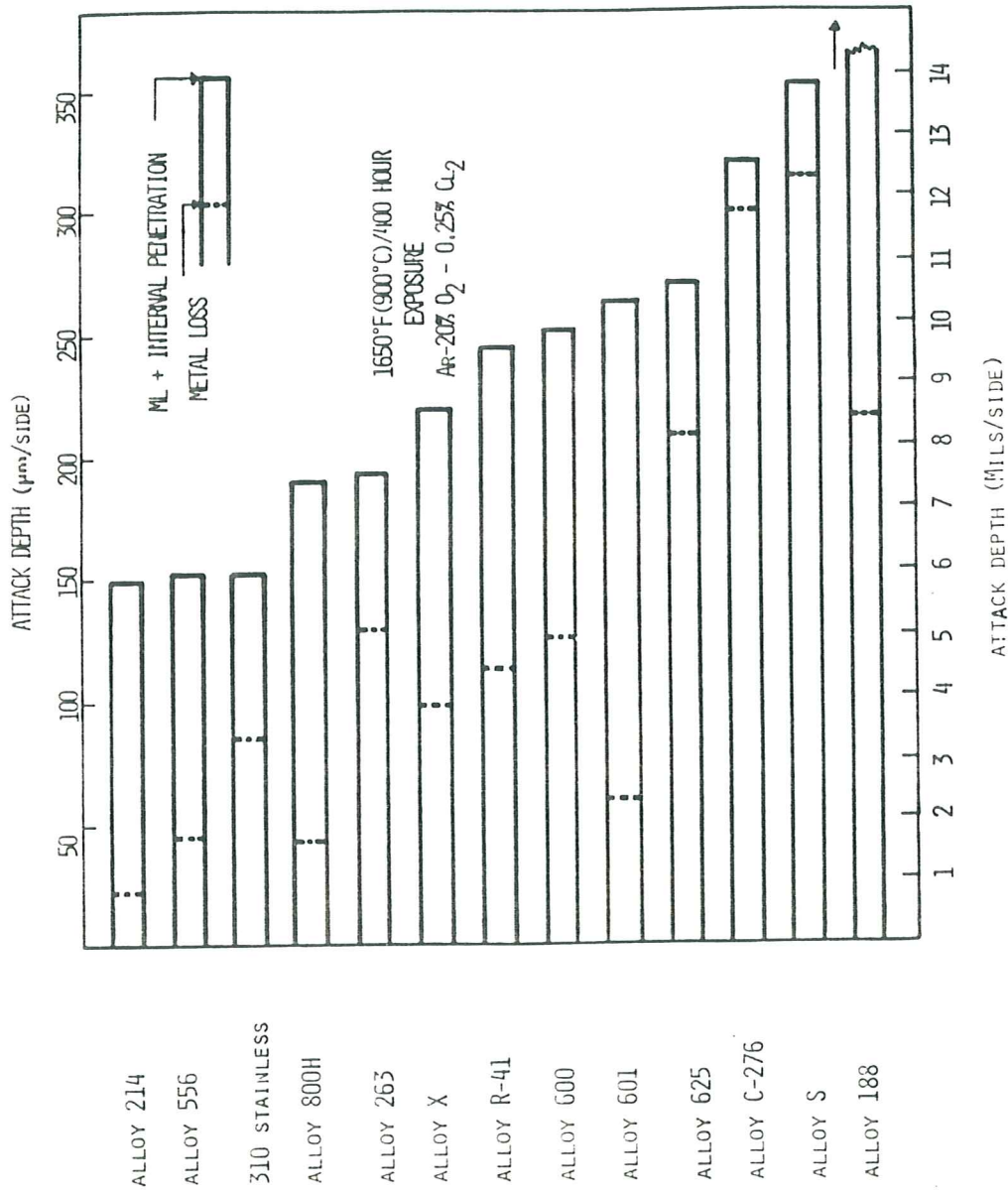


Figure 10. Metal wastage and internal penetration of specimens after 400 hours of exposure determined from optical micrographs.

specimen. CABOT alloy number 214 shows the best performance followed by the iron based alloys, and the alloys which are high in refractory metals show the most severe attack.

Figure 11 shows a scanning electron micrograph from a region of the cross section of the INCONEL alloy No 601 specimen near the surface where the internal attack can be seen clearly. The metal near the corroded surface is depleted of aluminum and chromium. The internal attack appears as open porosity, but the possibility that the attack occurs by internal formation of condensed chlorides cannot be ruled out because the samples were prepared by wet polishing, and the chlorides could have dissolved during polishing. The oxide scale on the specimen is rich in aluminum and chromium, and a small amount of chlorine can be detected in region 2 between the scale and the metal.

The scale which forms on INCONEL alloy No. 601 is not sufficiently protective to prevent the volatilization of chloride species from the specimen. CABOT alloy No. 214, which does contain sufficient aluminum to reduce the rate of volatilization from the specimen, is also subject to internal attack as shown in Figure 12. The oxide scale is rich in  $Al_2O_3$  and the metal near the surface is depleted in aluminum. The region of internal attack is also enriched in aluminum, suggesting that both internal chloridation and internal oxidation may be occurring.

#### Summary and Conclusions

1. Long term experiments on the corrosion of high temperature alloys in oxygen-chlorine environments generally confirm the trends observed in shorter term experiments.
2. Corrosion occurs by two mechanisms in this environment: Metal loss by formation of volatile chlorides and oxychlorides and internal attack.
3. CABOT alloy No. 214, which forms an aluminum oxide protective scale, shows the least corrosion in this environment, followed by the iron based alloys HAYNES alloy No. 556, 310 stainless steel, and alloy 800H. Alloys which are high in refractory metals, including HAYNES alloy No. 188, alloy 625, and HASTELLOY alloys S and C-276, experience the most severe corrosion in this environment, presumably because of the formation of volatile refractory metal oxychlorides.

#### References

1. H.H. Krause, D.A. Vaughan, P.D. Miller, 'Corrosion and Deposits from Combustion of Solid Wastes - Part 2 - Chloride Effects on Boiler Tube and Scrubber Metals' Trans ASME, Journal of Engineering for Power, 1974, Vol 96, pp 216-222
2. G. Marsh, P. Elliott, 'Oxidation of Some Nickel Containing Alloys in PVC Decomposition Products,' High Temperature Technology, 1982, Vol 1, pp 115-116
3. A. L. Plumley, W.R. Roczniak, 'Naturally Occurring High Chloride Coal and Superheater Corrosion - A Laboratory Study,' Trans ASME, Journal of Engineering for Power, 1982, Vol 104, pp 874-884



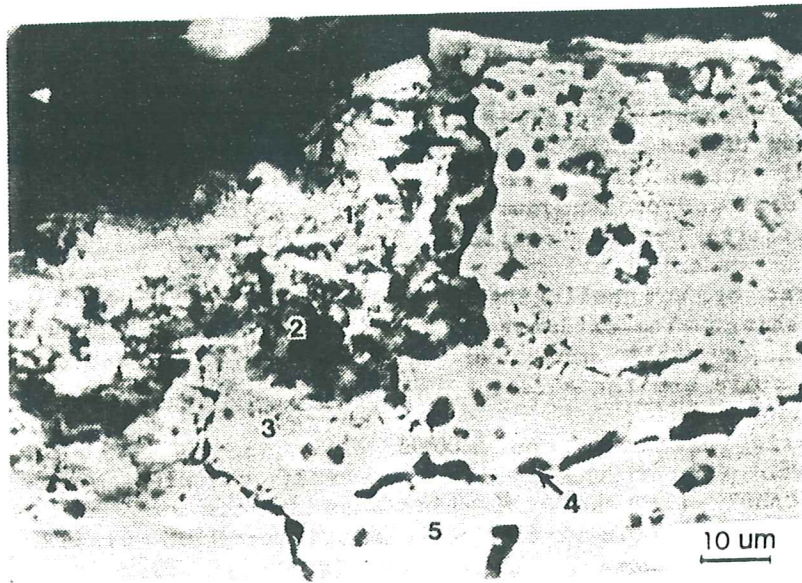


Figure 11. Scanning electron micrograph of cross section of INCONEL alloy 601 specimen near surface region showing internal attack. Semi-quantitative energy dispersive X-ray analyses

Position	%Al	%Cr	%Fe	%Ni	%Ti	%Si	%Cl
1	9.92	58.36	7.11	3.42	21.13	-	-
2	5.71	47.80	17.15	17.36	8.72	2.11	1.08
3	0	19.75	14.56	65.46	-	-	-
4	0.82	15.43	22.20	61.27	-	-	-
5	0.11	26.69	18.17	54.49	0.19	-	-

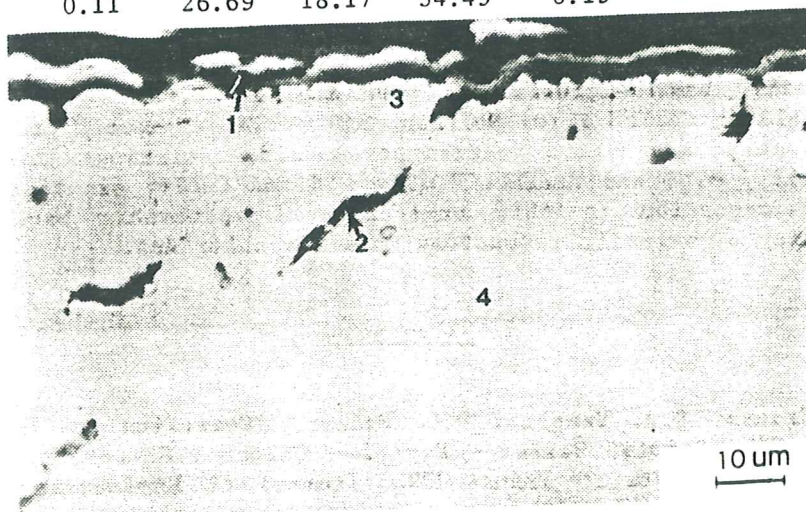


Figure 12. Scanning electron micrograph of cross section of CABOT alloy No. 214 specimen near surface showing internal attack. Semi-quantitative X-ray analyses.

Position	%Al	%Cr	%Fe	%Ni	%Ti
1	70.81	13.54	1.88	13.08	0.60
2	32.17	20.06	2.59	44.88	0.13
3	3.49	17.82	3.94	74.08	0.47
4	0.85	21.45	3.99	73.09	0.39

4. C.J. Dobos, W.W. Liang, 'High Temperature Materials for Gas Fired Industrial Applications,' pp 401-407 in Proceedings, Symposium on High Temperature Materials Chemistry-II, Z.A. Munir and D. Cubicciotti, Eds, The Electrochemical Society, Inc., Pennington, N.J. 1983
5. M.J. McNallan, W.W. Liang, J.M. Oh, C.T. Kang, 'Morphology of Corrosion Products Formed on Cobalt and Nickel in Argon-Oxygen-Chlorine Mixtures at 1000 K,' Oxid Metals, 1982, Vol 17, pp 371-389
6. A.S. Kim, M.J. McNallan, W.W. Liang, 'Oxidation of Cobalt-Chromium Alloys in Chlorine Contaminated Environments,' pp 266-277 in Proceedings, Symposium on High Temperature Materials Chemistry - II, Z.A. Munir and D. Cubicciotti Eds, The Electrochemical Society, Inc, Pennington, N.J., 1983
7. M.J. McNallan, C.T. Kang, W.W. Liang, 'Chlorination of Cobalt in an Argon-1 Pct Oxygen-1 Pct Chlorine Mixture at 1000 K,' Metall Trans, 1984, Vol 15A, pp403-405
8. R.P. Viswanath, D. Rein, K. Hauffe, 'High Temperature corrosion of NiCrAl Alloy in Oxygen-Chlorine Mixtures,' Werkst u Korros, 1980, Vol 31, pp 778-782
9. Y. Ihara, H. Ohgame, K. Sakayama, K. Hashimoto, 'The Corrosion Behavior of Fe-Ni Alloys in Hydrogen Chloride Gas and Gas Mixtures of Hydrogen Chloride and Oxygen at High Temperatures,' Trans, Japan Institute of Metals, 1982, Vol 23, pp 682-692
10. M.K. Hossain, J. E. Rhoades-Brown, S.R.J. Saunders, 'Measurement of Corrosion Rates of Commercial Alloys in HCl Gas at 400° C - 700° C,' in Proceedings UK CORROSION 83, Institute of Corrosion Science and Technology, 1983
11. S. Baranow, G.Y. Lai, M.F. Rothman, J.M. Oh, M.J. McNallan, M.H. Rhee, 'Materials Performance in High Temperature Halogen Bearing Environments,' paper number 16, CORROSION/84, National Association of Corrosion Engineers, Houston, Texas, 1984
12. Y.Y. Lee, M.J. McNallan, W.W. Liang, 'Kinetics of High Temperature Corrosion of Nickel in Ar-O<sub>2</sub>-Cl<sub>2</sub> Mixtures,' Presented at 113th AIME Annual Meeting, Los Angeles, CA, 1984
13. M.J. McNallan, M.J. Maloney, Y.Y. Lee, 'Kinetics of Mixed Oxidation of Nickel and Cobalt in Argon-Oxygen-Chlorine Environments,' Presented at 165th meeting of The Electrochemical Society, Cincinnati, Ohio, May 1984